AIAA JOURNAL
Vol. 34, No. 5, May 1996

Laser Doppler Anemometer Measurements of Turbulent Boundary Layer over a Riblet Surface

L. Djenidi* and R. A. Antonia†
University of Newcastle, Newcastle, New South Wales 2308, Australia

Laser Doppler anemometer measurements in a turbulent boundary layer downstream of a change from a smooth wall to a V-grooved riblet surface provide some insight into the way the near-wall turbulence structure adjusts to the new boundary condition. Depending on the riblet dimensions, this adjustment results either in drag reduction or drag increase. In the former case ($s^+ \lesssim 25$, where s is the distance between neighboring riblet tips and + denotes normalization by wall variables), the turbulence structure is essentially similar to that on a smooth wall. There are major structural differences in the latter case ($s^+ \geq 25$). Although near-wall secondary motions occur in both cases, the motions are much weaker when the riblets act to reduce the drag.

Nomenclature

b_{ij}	= Reynolds stress anisotropy tensor
C	= additive constant in logarithmic law
d	= average diameter of the quasistreamwise vortices
h	= riblet height
R_θ	= Reynolds number based on U_1 and θ
s	= riblet spacing
U_1	= freestream velocity
U_τ	= friction velocity
$\bar{U}, \bar{V}, \bar{W}$	= mean velocities in x, y, z directions, respectively
u, v, w	= velocity fluctuations in x, y, z directions, respectively
x, y, z	= streamwise, wall normal, and spanwise directions, respectively
y_0	= initial origin
δ	= boundary-layer thickness
δ_{ij}	= Kronecker symbol
θ	= momentum thickness
ν	= kinematic viscosity
$-\mathrm{II}$	= $(b_{ij}b_{ji})/2$
III	= $(b_{ij}b_{jk}b_{ki})/3$
$()^+$	= value nondimensionalized by U_1 and ν
$()'$	= root-mean-square value

I. Introduction

THE quasiorganized motion in the near-wall region of a turbulent boundary layer is known to play a major role in turbulent transport, and consequently significant effort has been directed towards controlling this motion mainly for the purpose of reducing the skin-friction drag. Both passive and active types of contol have been tried. As a passive means of control, riblets (longitudinal grooves at the wall) can, under certain conditions, reduce the frictional drag.[1] Although an impressive amount of information has been collected on the quasiorganized motion in a turbulent boundary layer over a smooth flat surface,[2] several issues remain unresolved. Robinson identified as key questions the dynamics of vortex formation and the interaction between coherent motions in the inner and outer regions of the layer. He also mentioned the need to look at noncanonical boundary layers to consider the effects of various parameters (pressure gradient, compressibility, wall roughness, wall curvature, etc.) on the turbulence structure. The replacement of a smooth wall with a riblet surface provides an interesting possibility for assessing how the nature of the boundary affects the quasiorganized motion. The fact that the same riblet surface can act either in a drag-reducing mode or a drag-augmenting mode only adds to this interest.

In previously published research on riblets, it has often been implied, if not directly stated, that riblets actually interact with the same quasiorganized motion that exists near a smooth wall. This implication is almost certainly inadequate since, for fully developed conditions, the near-wall turbulence structure should have adjusted to the wall geometry. In this context, any description of the riblets as acting on the turbulent vortical structure is strictly inappropriate. It would be more appropriate to think in terms of the turbulence structure adjusting to the riblet wall; previous descriptions of the interaction between riblets and the overlying vortical structures should be interpreted in this perspective.

There have been many studies, both qualitative and quantitative, dealing with the turbulence structure over riblets (see Walsh[3] for a review). Visualizations have indicated only small, if any, structural changes between riblet flows and smooth surface flows. In particular, low-speed streaks, similar to those observed on a smooth wall, occur over riblets. There is, however, no concensus about the magnitude of the mean streak spacing over riblets. Similarly, there is no agreement on the behavior of skewness and flatness factor of velocity fluctuations. It is possible that this general lack of agreement reflects possible differences in the experimental conditions under which different riblet experiments have been carried out. Recently, particle image velocimetry[4] (PIV) and direct numerical simulation[5] (DNS) data have emphasized the need to distinguish between drag-reducing and drag-augmenting riblet surfaces. These studies have also provided important detailed information on how conventional turbulence quantities are affected by the riblets. Further, the DNS data have highlighted the presence of near-wall quasistreamwise vortices that are geometrically similar to those over a smooth wall. However, since the primary focus of these studies has not been on quasicoherent structures, the possibility of gaining insight into the near-wall quasiorganized motion has received less attention. Consequently, the re-examination of existing data with this perspective in mind could be helpful as would further studies that may shed some light on whether or not there are genuine differences in the structure of turbulent boundary layers over riblet and smooth walls.

The present study is part of a more general experimental program that aims at providing information on the effects of different surface conditions on a turbulent boundary layer. Laser Doppler anemometry (LDA) is used for investigating the manner in which the flow structure adapts to the riblet surface. The main interest is on the near-wall region, where the Reynolds stresses can, under certain conditions, differ significantly from those on a smooth wall.

II. Experimental Facility and Conditions

A closed circuit constant-head water tunnel was used.[6] The 2-m-high vertical working section (250 × 250 mm) is made of 20-mm-thick perspex. One of the working section walls, which is removable,

Received Dec. 27, 1994; revision received May 30, 1995; accepted for publication July 24, 1995.

*Lecturer, Department of Mechanical Engineering.
†Professor, Department of Mechanical Engineering. Member AIAA.

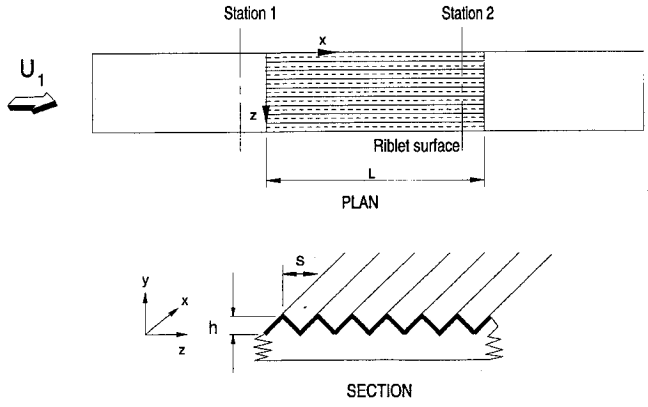

Fig. 1 Geometry of the surface. The origin for x is taken at the leading edge of the riblet surface.

was used as the smooth wall. A roughness strip, made up of 4.5-mm-high pebbles glued onto a 30-mm-wide perspex strip, was recessed into a groove about 100 mm downstream from the exit of the contraction and used to trip the boundary layer. The measurement station was located about 1 m downstream of the roughness strip. The injection of dye through a hole in the wall indicated that the boundary layer is turbulent at this station when the freestream velocity U_1 exceeds about 8 cm/s. The maximum freestream velocity was about 50 cm/s and the freestream turbulence intensity was about 0.5%. The boundary-layer thickness δ was in the range of 30–50 mm, leaving a sufficient core of irrotational flow. The pressure gradient was checked by measuring U_1 at several axial locations and found to be negligibly small ($U_1\, dU_1/dx = 5.5 \times 10^{-4}$ ms^{-2} for $U_1 \approx 22$ cm/s).

The riblet surface was integrated into the removable wall, with the riblet crest plane being adjusted so that it was flush with the upstream and downstream smooth surfaces (Fig. 1). The riblets consisted of 0.3-m-long longitudinal triangular cross-sectional grooves, covering the full width of the working section. The riblet height and the spacing between adjacent riblet tips were equal to 2.6 and 6 mm, respectively. The leading edge of the riblet plate was 1.2 m downstream from the roughness strip.

Measurements were made on the smooth wall at $X = -50$ mm (station 1) and over the riblets at $X = 250$ mm (station 2) for $U_1 = 8$ cm/s (at $X = -50$ mm, $R_\theta = 3.6 \times 10^2$ and $\delta = 53$ mm) and $U_1 = 25$ cm/s ($R_\theta = 7.65 \times 10^2$ and $\delta = 37$ mm). Under these conditions, $h^+ = 11$ and $s^+ = 25$ ($R_\theta = 3.6 \times 10^2$), and $h^+ = 30$ and $s^+ = 71$ ($R_\theta = 7.65 \times 10^2$). Earlier work[3] suggests that the former (h^+, s^+) combination should yield a drag reduction, whereas the latter should result in drag augmentation. The smooth wall data at $R_\theta = 3.6$ and 7.65×10^2 compared well with the DNS of Spalart[7] (not presented here). Also, flow visualization showed that, for the present conditions, the flow was fully turbulent at $R_\theta = 3.6 \times 10^2$ (see Ref. 6).

The water-tunnel geometry allowed a three-component fiber optic LDA system (5W argon-ion) to be used mainly in forward scattermode. The backscatter mode was used only to obtain w. Only two-component ($u - v$) (two pairs of beams, each pair measuring one component) and one-component (w) (one pair of beams) measurements were made. The measuring volume dimensions were $0.04 \times 0.04 \times 0.5$ and $0.04 \times 0.04 \times 0.9$ mm for the two- and one-component measurements, respectively. For the forward scatter ($u - v$) measurements, the measuring volumes had their largest dimension (about 2 and 3.6 wall units) parallel to the riblet crest plane. Backscatter was used for the w measurements, the measuring volume having its largest dimension (about two wall units) in a direction perpendicular to the riblet crest plane. The measured and physical axes were parallel to each other, and it was therefore unnecessary to apply a coordinate transformation to the data. Enhanced burst spectrum analyzers (BSAs) were used for processing the photomultiplier signals. Typical data rates in the outer part of the layer were about 200 Hz, falling off to about 10 Hz close to the wall. In the outer layer, 10,000 samples were collected at each measurement point; this was reduced to 3000 samples close to the wall. Analog outputs from the BSAs were digitized into a personal computer and stored for subsequent data reduction and analysis. Checks were made of the convergence of the velocity moments (up to order 4) by plotting the integrands $u^n p(u)$ [$p(u)$ is the probability density function of u]. The results (not presented here) showed satisfactory convergence, pointing out that the measurements were reliable.

III. Results and Discussion

A. Smooth Wall

Before considering the boundary-layer flow over the riblets, it is important to ascertain the quality of LDA measurements over a smooth wall. The latter measurements provide a basis for comparison with the riblet surface measurements. The measured normalized mean velocity distribution ($R_\theta = 1.4 \times 10^3$) is compared in Fig. 2 with the DNS distribution at $R_\theta = 1.41 \times 10^3$ of Spalart.[7] The friction velocity used for normalizing the data was deduced from the measured mean velocity gradient in the region $y^+ \leq 2.5$ (for details see Djenidi and Antonia[8]). There is good agreement everywhere in the layer. Agreement of similar quality is observed (Fig. 3) for the turbulence intensities and the Reynolds shear stress. The spanwise velocity fluctuation could not be measured below $y^+ = 30$ because of the particular beam configuration that was used and the problem caused by wall reflections. The agreement between DNS and measured profiles of v'^+ and $-\overline{u^+v^+}$ is especially encouraging.

B. Riblet Surface

1. Mean Velocity Measurements

Mean velocity distributions over the riblet surface (at the crest and trough) for $s^+ = 25$ and 71 ($R_\theta = 3.6$ and 7.65×10^2, respectively) are shown in Fig. 4 (a semilogarithmic scale is used). The smooth wall data are also shown. The origin for the riblet velocity profiles is taken at the riblet trough. The present data (at $s^+ = 25$) compare well (see Fig. 4b, where the origin of the distributions is taken along the riblet contour) with the hot-wire data of Vukoslavcevic et al.[9] ($s^+ = 34$ and $R_\theta = 1.0 \times 10^3$). Note that the ($u - v$) measurement

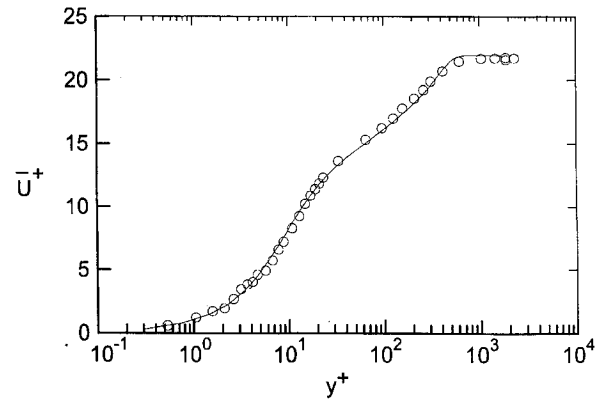

Fig. 2 Longitudinal mean velocity profile: ○, experiment and ——, DNS data.[7]

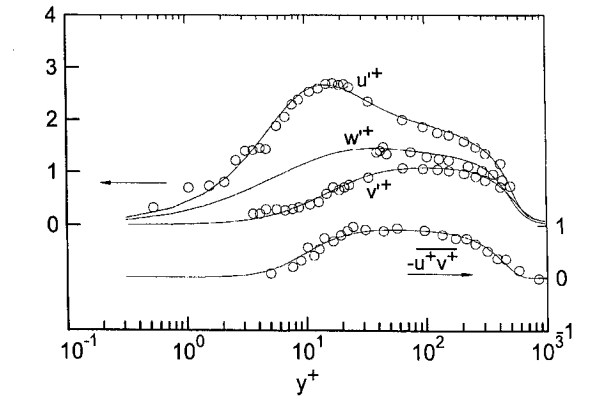

Fig. 3 RMS u, v, and w and Reynolds shear stress profiles: ○, experiment and ——, DNS data.[7]

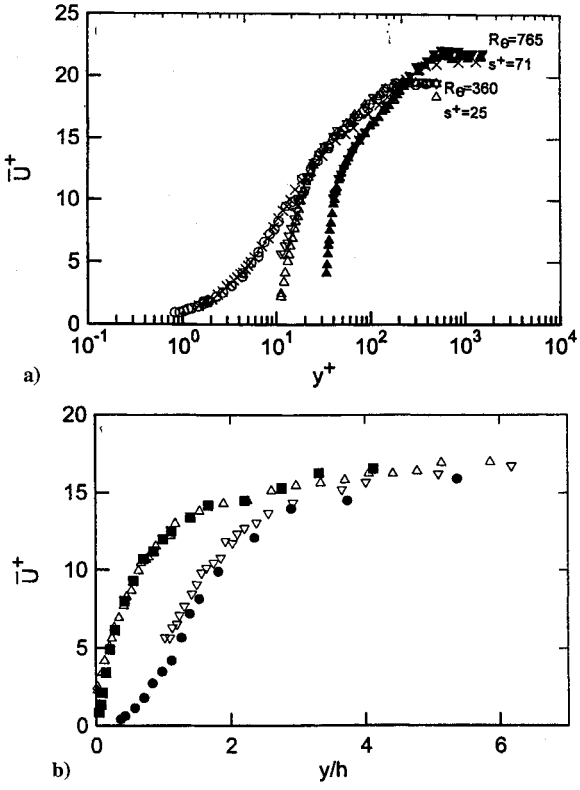

Fig. 4 Longitudinal mean velocity profiles. The origin is taken at the riblet trough: a) ○ and ×, smooth wall; ▽ ($s^+ = 25$ and $R_\theta = 3.6 \times 10^2$) and ▼ ($s^+ = 71$, and $R_\theta = 7.65 \times 10^2$), riblet trough; and △ ($s^+ = 25$) and ▲ ($s^+ = 71$), riblet tip; and b) close symbols, Vukoslavcevic et al.[9]; $y/h = 0$ is taken along the riblet contour.

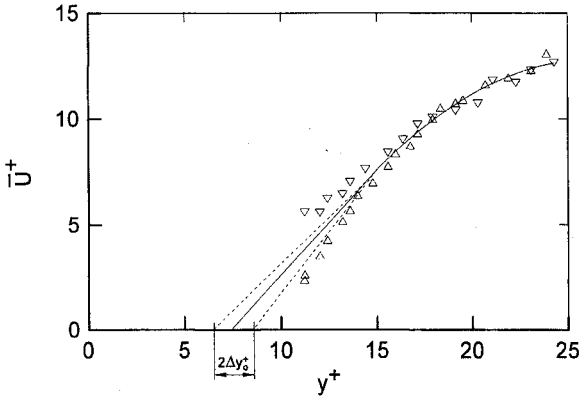

Fig. 5 Determination of the virtual origin y_0. Symbols same as for Fig. 4 and ——, interpolated mean velocity.

mode (cf. Sec. II) prevents measurements in the riblet valley. All data have been normalized with the smooth wall friction velocity.

There is no spanwise variation in $\bar{U}^+$ for $y^+ \geq 20$ (a distance of about one riblet height above the riblet crest plane) when $s^+ = 25$ and $y^+ \geq 45$ (about half a riblet height above the crest plane) when $s^+ = 71$. Only in the viscosity-dominated region near the riblet wall can a spanwise variation be discerned. These observations are in agreement with previous experimental[9] and DNS[5] data. This suggests a two-layer model for the flow: a relatively thick turbulent layer sliding over a much thinner viscous layer.[10] The former layer is apparently unaware of the geometrical inhomogeneity of the wall and is virtually two dimensional. This in turn suggests that the possible use of a virtual or fictitious smooth wall may be helpful for comparing riblet and smooth wall flows. Choi et al.[5] tested four definitions of virtual origins for riblets and found that only two were appropriate at low Reynolds numbers. The first is that of Bechert and Bartenwerfer.[11] The second, defined by Choi et al., is based on changes in the turbulence structure. Since these two origins were

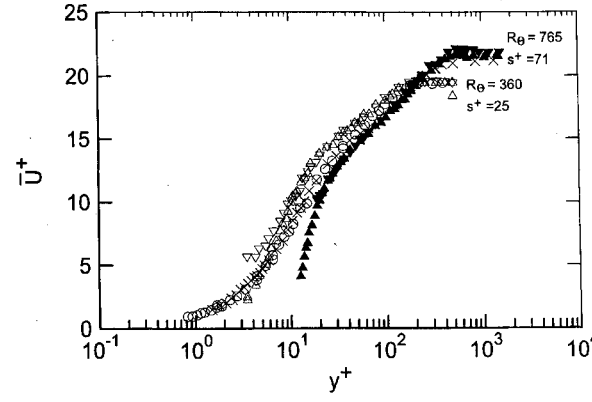

Fig. 6 Longitudinal mean velocity profile; $y_0 = 0$ is the virtual origin. Symbols same as for Fig. 4.

almost identical, we have opted to use Bechert and Bartenwerfer's origin, mainly because it can be applied easily.

Assuming that the riblets are immersed within the viscous sublayer, Bechert and Bartenwerfer defined the virtual (or average) origin y_0 as the origin of the spanwise averaged velocity profiles. To estimate y_0 experimentally, the velocity profiles (such as in Fig. 4) are linearly extrapolated from the point where they first diverge down to $\bar{U} = 0$ on the y axis (see Fig. 5). The intersection defines the virtual origin. Bechert and Bartenwerfer used conformal mapping to determine y_0. The virtual origin experimentally obtained in Fig. 5 ($s^+ = 25$) is about $y_0^+ = 7.5$ (±1%), whereas the theoretical value is 7.7. For $s^+ = 71$, the theory of Bechert and Bartenwerfer may not be appropriate since the riblets extend beyond the viscous sublayer. However, the location of the actual virtual origin must lie between the riblet tips and the virtual origin ($y_0^+ = 19$) obtained experimentally using the preceding method. The LDA data of Fig. 4 are replotted in Fig. 6, where y is measured from the virtual origin. Clearly, there is a region above the riblet surface where, relative to the smooth wall, the velocity is increased when $s^+ = 25$ and reduced for $s^+ = 71$. This region extends to $y^+ = 150$ and 100 in the former and latter configurations, respectivley. It should be underlined that the streamwise fetch over the riblet surface is short; consequently, the internal layer associated with the smooth to riblet surface junction has not yet reached the edge of the upstream boundary layer at $X = 250$ mm. Choi,[12] Choi et al.,[5] and Benhalilou et al.[13] also noted a higher velocity region above the riblet surface.

The relatively large extent of this region suggests that the riblets affect the mean velocity in the outer region of the layer. This can be interpreted in the context of the two-layer model: when $s^+ = 25$, the turbulent layer slides over the viscous layer at a faster rate than over a smooth wall; the inverse occurs when $s^+ = 71$. Such behavior may be associated with an increase (decease) of the viscous sublayer thickness. The change in the viscous sublayer thickness is interpreted as a change in the additive constant C in the logarithmic law (Bradshaw[10]): an increase of C corresponds to frictional drag reduction and vice versa. The drag-reducing configuration should then result in the logarithmic velocity region over the riblet surface being displaced above that over a smooth wall (increase in C), as shown, for example, by Hooshmand et al.[14] and Baron and Quadrio.[15] This upward shift, however, is not evident in Fig. 4 or Fig. 6, but it should be recalled that the data in these figures are normalized by the smooth wall friction velocity; also, there is strictly no logarithmic region when R_θ is small. It is perhaps also useful to recall that for low Reynolds numbers the separation between small and large length scales is less distinct than at high Reynolds numbers. Particularly, in turbulent boundary layers at low R_θ, inner and outer scales overlap significantly.[7,8] Consequently, the present low-Reynolds-number results must be treated with caution. For example, although high and low R_θ turbulent boundary layers may have geometrically similar turbulence structures, the interaction and relative importance of these structures may well change with R_θ. For this reason, one should, perhaps, consider the present (and indeed all existing low R_θ) data as providing a qualitative description only of a turbulent boundary layer over riblets.

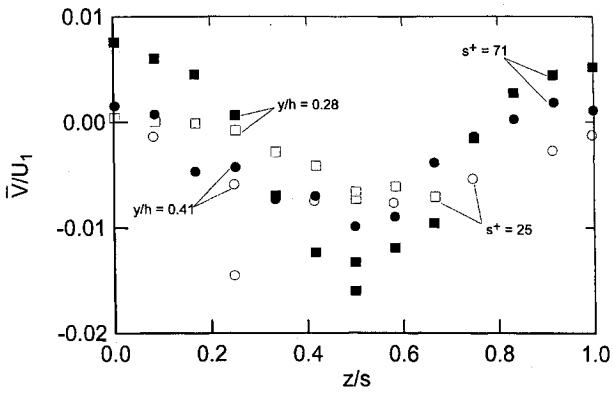

Fig. 7 Spanwise variation of normal mean velocity over riblets, y/h = 0.28: □, s^+ = 25 and ■, s^+ = 71; and y/h = 0.41: ○, s^+ = 25 and ●, s^+ = 71.

2. Mean Secondary Flow Measurements

Since near-wall riblet flows have geometrical features that are similar to those of corner flows, it is of interest to ascertain whether there are mean secondary motions within or near the riblet canopy. From a turbulence modeling viewpoint, the possible existence of secondary motions is important. Except for the PIV measurements of Suzuki and Kasagi,[4] only numerical studies[5,16–18] have shown evidence of mean secondary flows over riblets.

Figure 7 shows the spanwise variation of $\bar{V}$ (the mean velocity component normal to the riblet crest plane) for $s^+ = 25$ and 71. Mean counter-rotating secondary-type flows can be discerned in the vicinity of the riblets. The apparent upward shift of the origin $\bar{V} = 0$—the data for $s^+ = 25$ and $y/h = 0.41$ are always negative—is probably due to a small deviation from orthogonality of the two laser beam pairs. This departure results in $\bar{V}$ being contaminated by $\bar{U}$ (Ref. 19).

The shape of the spanwise distributions suggests that the centers of the counter-rotating motions are located at $z/s = 0.25$ for $s^+ = 25$ and 0.75 for $s^+ = 71$, i.e., midway between the tip and the trough. This is in agreement with the DNS data of Choi et al.[5] The direction of the counter-rotating motion is in accord with the DNS and PIV data of Suzuki and Kasagi.[4] Momentum is convected towards ($\bar{V} < 0$) the riblet valley and away ($\bar{V} > 0$) from the valley along the riblet contour. For $s^+ = 25$, the intensity of the motion is much weaker than for $s^+ = 71$. It may be argued that, for $s^+ \leq 25$ and more generally for drag-reducing conditions, this secondary motion is weak enough to be neglected in computations.[20]

3. Reynolds Stress Measurements

Distributions of u'^+ and v'^+ over the riblets (tip and trough) are compared with those over the smooth wall in Fig. 8a ($s^+ = 25$) and Fig. 8b ($s^+ = 71$). In Fig. 8a, the w'^+ distributions above the riblet trough and the w'^+ DNS data of Spalart[7] at $R_\theta = 3.0 \times 10^2$ are also shown. The data have been normalized by the smooth wall friction velocity. For the riblet data, $y^+ = 0$ is the virtual origin deduced from the mean velocity distributions (see Fig. 5). When $s^+ = 25$, there is no significant difference between the riblet and smooth wall data for v'^+ and w'^+. At $y^+ \approx 13$, the peak value of u'^+ above the riblet trough is about 6% smaller than on the smooth wall, whereas, above the riblet crest, it is indistinguishable from the smooth wall value. When $s^+ = 71$, u'^+ and v'^+ are increased (relative to the smooth wall) over the crest and reduced over the trough for $y^+ \leq 40$; note, however, that v'^+ appears to be less affected than u'^+. For $y^+ \geq 40$, the riblet data are higher than those on a smooth wall, regardless of the spanwise location. This is in agreement with the previously cited experimental and DNS data.

The $-\overline{u^+v^+}$ data for $s^+ = 25$ (Fig. 9a) are significantly different from those for $s^+ = 71$ (Fig. 9b) in the near-wall region. For $s^+ = 25$, the maximum value of $-\overline{u^+v^+}$ over either tip or trough is about 25% smaller than on the smooth wall. For $s^+ = 71$, the peak value of $-\overline{u^+v^+}$ over the riblet tip is about 15% larger than on the smooth wall, whereas there is no substantial difference between the peak values over the riblet trough and the smooth wall. In both

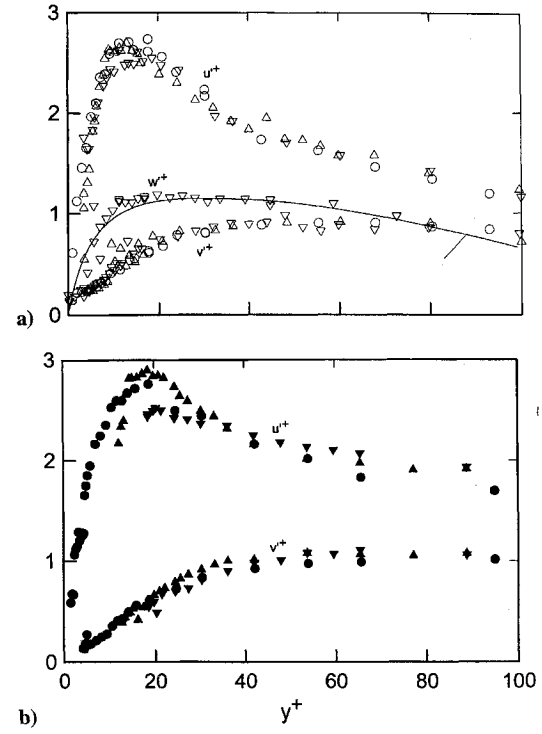

Fig. 8 RMS u, v, and w distributions: a) s^+ = 25, and b) s^+ = 71. Symbols same as for Fig. 4; ●, smooth wall; and ——, DNS data.[7]

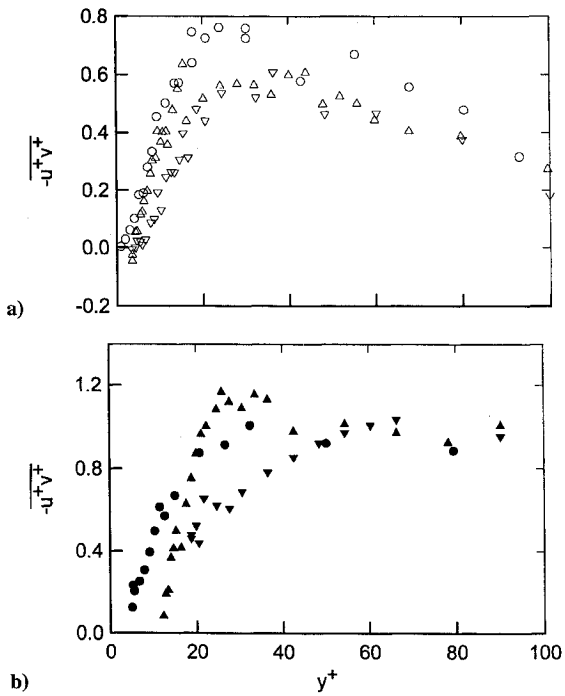

Fig. 9 Reynolds shear stress distributions: a) s^+ = 25, and b) s^+ = 71. Symbols same as for Fig. 8.

configurations, the data merge with the smooth wall distribution for $y^+ \geq 100$. Near the riblet wall, the spanwise variation of $-\overline{u^+v^+}$ is greater for $s^+ = 71$ than $s^+ = 25$. These results are consistent with the DNS data of Choi et al.,[5] which show that sweep (fourth-quadrant) and ejection (second-quadrant) motions, i.e., the major contributors to $-\overline{uv}$, are sensitive to the riblets. When $s^+ = 20$ (drag-reducing condition), contributions from sweeps and ejections have nearly the same magnitude as on a smooth wall; when $s^+ = 40$ (drag-augmenting condition) they differ significantly from a smooth wall. The DNS data also suggest that events associated with the first and third quadrants are nearly unchanged, relative to the smooth wall.

The differences in u'^+, v'^+, and $-\overline{u^+v^+}$ between $s^+ = 25$ and 71 are similar to those observed for the DNS data.[5] Such differences are also found in other experimental data (Benhalilou et al.[13]). The DNS data also indicate that the spanwise variations of v'^+ and w'^+ extend into the region where there is no noticeable spanwise variation of u'^+ (this can be discerned in the present LDA data of u'^+ and v'^+ when $s^+ = 71$). Choi et al. argued that this implied a greater sensitivity of the cross flow than the streamwise flow to the riblets. Apparently, the riblets affect the spanwise motion to a greater degree than the streamwise motion.

Although the spanwise variation of $\bar{U}^+$ over riblets disappears at $y^+ \approx 10$ for $s^+ = 25$ and $y^+ \approx 30$ for $s^+ = 71$ (see Fig. 6a), the corresponding variation of $-\overline{u^+v^+}$ vanishes at $y^+ \approx 30$ ($s^+ = 25$) and 60 ($s^+ = 71$). The same trend is observed in the DNS data between $s^+ = 20$ and 40. This implies that the turbulence field is more sensitive to the wall condition than the mean field. Further, the significant changes that occur in the Reynolds stresses between $s^+ = 25$ and 71 ($s^+ = 20$ and 40 for the DNS) may reflect the effect of the response of the layer to changes in the riblet dimensions. Arguably, the extent of the riblet-affected region is a measure of this response. Changes in the Reynolds shear stress suggest changes in $-\overline{uv}\partial\bar{U}/\partial y$, the average production of turbulent kinetic energy (the contribution from other production terms, such as $-\overline{uw}\partial\bar{U}/\partial z$, for example, is negligible.[5,21,22] This, in turn, would result in changes to the balance between the average energy production and dissipation rates.

The different behaviors of the Reynolds stresses for $s^+ = 25$ and 71 and the extent of the region where changes occur suggest that the turbulence-producing structures of the flow may play an important role in drag reduction. Kim[23] and Choi et al.[5] argued that, since the average diameter d^+ of the intense quasistreamwise vortices near a smooth wall is about 30 (e.g., Refs. 2 and 24), these vortices will have more difficulty penetrating the riblet valley when $s^+ = 20$ than when $s^+ = 40$. Consequently, a much smaller area is exposed to the vortex-induced downwash when $s^+ = 20$ than when $s^+ = 40$, resulting in drag reduction and augmentation in the former and latter cases, respectively. As noted in the Introduction, this explanation is not entirely satisfactory since it implicitly assumes that riblet and smooth wall flows have quasistreamwise vortices of comparable intensity. Suzuki and Kasagi[21] noted that, for drag-reducing conditions, the riblet valley may act as a free-slip surface to the streamwise vortices, thus reducing the possibility of vortex regeneration (in contrast to the likelihood of regeneration through a no-slip boundary). A further effect that may be at play in a drag-reducing situation is the dominance of viscous effects in the riblet valley where all quantities are strongly damped. These viscous effects account for the observation that, in laminar flows, there is no difference in the frictional drag between a smooth surface and a riblet surface.[3,25,26] It is conceivable that, in turbulent flows, viscous effects can beneficially complement the role played by the overlying quasistreamwise vortives in drag-reducing conditions. Djenidi and Antonia[20] have further conjectured that viscous effects may put a brake on the expected drag increase when s^+ is sufficiently large to allow the vortices to penetrate the riblet valley.

Other drag-reducing mechanisms have been proposed, some of them overlapping the previous proposal. For example, Bacher and Smith[27] recognized as significant the fact that the most successful drag-reducing wall geometry has dimensions comparable to the size and spacing of the longitudinal counter-rotating vortices observed on a smooth wall. The DNS data[2] provide only weak evidence for counter-rotating vortices, implying that the spacing between vortices should not be an important parameter in the context of drag reduction. Bacher and Smith suggested that the riblet peak plays a major role in weakening the longitudinal vortices. The effective removal of the no-slip surface could, however, be just as important in reducing the vorticity of these vortices. It has also been suggested[12,27,28] that the riblets inhibit the spanwise motion of the vortices.

All of the previous observations (LDA and DNS data) are consistent with the notion that near-wall quasistreamwise vortices over riblets have similar geometrical features to those near a smooth wall. However, depending on whether the riblet configuration is a drag-reducing or drag-augmenting one, different equilibrium conditions exist. In support of this are the DNS data[12] showing that, relative

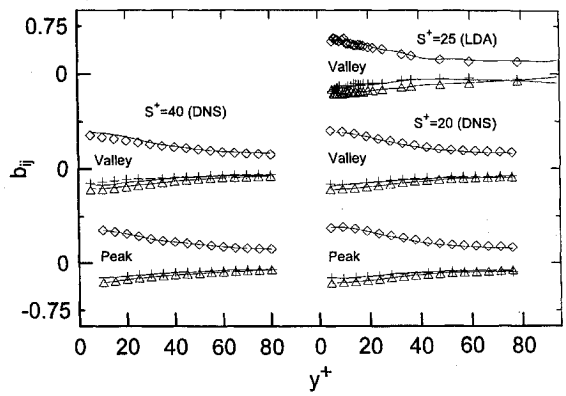

Fig. 10 Components of the Reynolds stress anisotropy tensor: ——, smooth wall; ◇, b_{11}; △, b_{22}; and +, b_{33}.

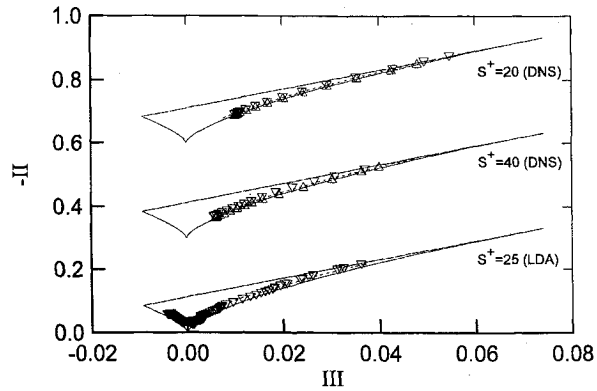

Fig. 11 Cross plot of second and third invariants of the Reynolds stress anisotropy tensor: - - - -, smooth wall; symbols same as for Fig. 4.

to a smooth wall, streamwise vorticity fluctuations above the riblets are weaker when $s^+ = 20$ and stronger when $s^+ = 40$. The outer riblet flow does not seem to be significantly different from that of a smooth wall flow. This suggests that the near-wall turbulence structure adjusts to the boundary conditions (the effective removal of the no-slip surface), resulting in either drag reduction or drag increase, depending on the dimensions of the riblets.

4. Reynolds Stress Anisotropy Tensor

The data examined in the previous section not only indicate changes to the magnitude of the Reynolds stresses but also point to possibly different intercomponent transfers of turbulent kinetic energy. Figure 10 shows distributions of the diagonal components of $b_{ij} = (\overline{u_iu_j}/\overline{u_iu_i} - \delta_{ij}/3)$ over the riblet trough ($s^+ = 25$) and over a smooth wall. The DNS data for $s^+ = 20$ and 40 have also been included in Fig. 10. No substantial difference is observed between the riblet and smooth wall data in the case of drag reduction. Very near the wall ($y^+ \leq 5$), there are marginal differences observed in the DNS data. The magnitudes of b_{11} and b_{33} are increased over the trough and reduced over the crest; b_{22} remains unchanged regardless of the spanwise position. These observations suggest that, for a drag-reducing configuration, the mechanism by which kinetic energy is distributed among its components should be quite similar to that for a smooth wall. Changes occur only within the viscous-dominated region near the riblet wall. There is therefore no significant structural change in the turbulence structure from that of a smooth wall. For drag-augmenting conditions, the DNS data show that the magnitudes of b_{11} and b_{33} are reduced in the region $y^+ \leq 30$ (b_{22} is less affected), suggesting changes in turbulence structure.

An effective way, invariant with respect to the choice of coordinate axes, of assessing the anisotropy of $\overline{u_iu_j}$ is to determine the invariants of b_{ij}. Plots of $-$II vs III of the LDA and DNS data of Fig. 10 are shown in Fig. 11. Note that this presentation does not require any knowledge of y or of its origin. Above the riblet trough, the LDA data exhibit little departure from the smooth wall data, whereas the DNS shows a tendency towards a one-component

state (the top vertex of the triangle). It would appear that the quality of the present riblet near-wall data may not be sufficiently high to reproduce this trend. Above the crest, the DNS data indicate no difference from the smooth wall. The trend of the DNS data would support the suggestion that the spanwise motion is less vigorous than on a smooth wall. When the riblets are operating in a drag-augmenting condition ($s^+ = 40$), the DNS data lie below those on a smooth surface, indicating a more isotropic state; the bottom cusp (II = III = 0) identifies the isotropic state. The data of Suzuki and Kasagi[21] exhibit the same trends as in Figs. 10 and 11.

IV. Conclusions

LDA data in a turbulent boundary layer over a riblet surface indicate that the influence of the surface on the near-wall turbulence structure differs, according to whether the riblets reduce or increase the skin-frictional drag by comparison to a smooth wall. The Reynolds stress tensor over drag-reducing riblets is only marginally different (except in the viscous-dominated region near the wall) from that on a smooth wall. On the other hand, for drag-augmenting conditions, the Reynolds stresses are larger and the flow is more isotropic than on a smooth wall. These features are generally consistent with previously published PIV and DNS data.[4,5]

A key factor in the process that brings about the changes appears to be an adjustment of the near-wall quasiorganized motion to the change in boundary conditions (effective removal of the no-slip surface). This adjustment depends critically on the riblet dimensions. For drag-reducing conditions, there should be no major structural difference in the quasiorganized motion. The quasistreamwise vortices are weaker than on a smooth wall, and their ability to transport momentum to the wall is less effective. The opposite is true for drag-augmenting configurations. In these conditions, the structural change extends some distance into the flow, possibly suggesting a relatively important level of communication between the wall region and the outer region. Arguably, the strength of the communication should reflect the vortical strength in the wall region.

Acknowledgment

The support of the Australian Research Council is gratefully acknowledged.

References

[1]Coustols, E., and Savill, A. M., "Turbulent Skin Friction Drag Reduction by Active and Passive Means, Special Course on Skin Friction Drag Reduction," AGARD Rept. 786, 1991, pp. 8.1–8.80.

[2]Robinson, S. K., "Coherent Motions in the Turbulent Boundary Layer," *Annual Review of Fluid Mechanics*, Vol. 23, 1991, pp. 601–609.

[3]Walsh, M. J., "Riblets," *Viscous Drag Reduction in Boundary Layers*, edited by D. M. Bushnell and J. N. Hefner, Vol. 123, Progress in Astronautics and Aeronautics, AIAA, Washington, DC, 1990, pp. 203–261.

[4]Suzuki, Y., and Kasagi, N., "Turbulent Drag Reduction Mechanism Above a Riblet Surface," *AIAA Journal*, Vol. 32, No. 9, 1994, pp. 1781–1790.

[5]Choi, H., Moin, P., and Kim, J., "Direct Numerical Simulation of Turbulent Flow over Riblets," *Journal of Fluid Mechanics*, Vol. 255, 1993, pp. 503–539.

[6]Ching, C. Y., Djenidi, L., and Antonia, R. A., "Low Reynolds Number Effects in a Turbulent Boundary Layer," *Experiments in Fluids*, Vol. 19, No. 1, 1995, pp. 61–68.

[7]Spalart, P. R., "Direct Simulation of a Turbulent Boundary Layer up to $R_\theta = 1410$," *Journal of Fluid Mechanics*, Vol. 187, 1988, pp. 61–98.

[8]Djenidi, L., and Antonia, R. A., "LDA Measurements in a Low Reynolds Number Turbulent Boundary Layer," *Experiments in Fluids*, Vol. 14, No. 4, 1993, pp. 280–288 (Erratum, *Experiments in Fluids*, Vol. 15, No. 4/5, 1993, p. 386)

[9]Vukoslavcevic, P., Wallace, J. M., and Balint, J. L., "Viscous Drag Reduction Using Streamwise-Aligned Riblets," *AIAA Journal*, Vol. 30, No. 4, 1992, pp. 1119–1122.

[10]Bradshaw, P., "Turbulence: The Chief Outstanding Difficulty of Our Subject," *Experiments in Fluids*, Vol. 16, No. 3/4, 1994, pp. 203–216.

[11]Bechert, D. W., and Bartenwerfer, M., "The Viscous Flow on Surfaces with Longitudinal Ribs," *Journal of Fluid Mechanics*, Vol. 206, 1989, pp. 105–129.

[12]Choi, K. S., "Effects of Longitudinal Pressure Gradient on Turbulent Drag Reduction with Riblets," *Proceedings of the 4th European Drag Reduction Meeting: Turbulence Control by Passive Means*, edited by E. Coustols, Kluwer, Dordrecht, The Netherlands, 1990, pp. 109–121.

[13]Benhalilou, M., Anselmet, F., and Fulachier, L., "Conditional Reynolds Stress on a V-grooved Surface," *Physics of Fluids*, Vol. 6, No. 6, 1994, pp. 2101–2117.

[14]Hooshmand, D., Youngs, R., and Wallace, J. M., "An Experimental Study of Changes in the Structure of a Turbulent Boundary Layer due to Surface Geometry Changes," AIAA Paper 83-0230, Jan. 1983.

[15]Baron, A., and Quadrio, M., "Some Preliminary Results on the Influence of Riblets on the Structure of a Turbulent Boundary Layer," *International Journal of Heat and Fluid Flow*, Vol. 14, No. 4, 1993, pp. 223–230.

[16]Khan, M. M. S., "A Numerical Investigation of the Drag Reduction by Riblet Surface," AIAA Paper 86-1127, May 1986.

[17]Launder, B. E., and Li, S. P., "On the Prediction of Flow over Riblets Via a 2nd-Moment Closure," *Near-Wall Turbulent Flows*, edited by R. M. S. So, C. G. Speziale, and B. E. Launder, Elsevier, Amsterdam, 1993, pp. 739–748.

[18]Tullis, S., and Pollard, A., "Modelling the Time Dependent Flow over Riblets in the Viscous Wall Region," *Applied Science Research*, Vol. 50, No. 3/4, 1993, pp. 299–314.

[19]Djenidi, L., Anselmet, F., and Antonia, R. A., "LDA Measurements in a Turbulent Boundary Layer over a d-type Rough Wall," *Experiments in Fluids*, Vol. 16, No. 5, 1994, pp. 323–329.

[20]Djenidi, L., and Antonia, R. A., "Riblet Modelling Using a Second Moment Closure," *Applied Science Research*, Vol. 54, No. 4, 1995, pp. 249–266.

[21]Suzuki, Y., and Kasagi, N., "On the Turbulent Drag Reduction Mechanism Above a Riblet Surface," AIAA Paper 93-3257, July 1993.

[22]Benhalilou, M., Anselmet, F., Fulachier, L., and Antonia, R. A., "Experimental Investigation of a Turbulent Boundary Layer Manipulated by a Ribbed Surface," *Proceedings of the 9th Symposium on Turbulent Shear Flows*, Vol. 1, Kyoto Univ., 1994, pp. P107.1–P107.4.

[23]Kim, J., "Study of Turbulent Structure Through Numerical Simulations: The Perspective of Drag and Reduction, Special Course on Skin Friction Drag Reduction," AGARD Rept. 786, 1991, pp. 7.1–7.14.

[24]Kim, J., Moin, P., and Moser, R., "Turbulence Statistics in Fully Developed Channel Flow at Low Reynolds Number," *Journal of Fluid Mechanics*, Vol. 177, 1987, pp. 133–166.

[25]Djenidi, L., and Antonia, R. A., "Numerical Study of Laminar Flows Over Riblets," Rept. TN-FM 94/1, Dept. of Mechanical Engineering, Univ. of Newcastle, New South Wales, Australia, 1994.

[26]Djenidi, L., Anselmet, F., Liandrat, J., and Fulachier, L., "Laminar Boundray Layer Over Riblets," *Physics of Fluids A*, Vol. 6, No. 9, 1994, pp. 2993–2999.

[27]Bacher, E. V., and Smith, C. R., "A Combined Visualization-Anemometry Study of the Turbulent Drag Reducing Mechanisms of Triangular Micro-Groove Surface Modifications," AIAA Paper 85-0548, 1985.

[28]Chu, D. C., and Karniadakis, G. E., "A Direct Numerical Simulation of Laminar and Turbulent Flow over Riblet-Mounted Surfaces," *Journal of Fluid Mechanics*, Vol. 250, 1993, pp. 1–42.